Excitation laser energy dependence of surface-enhanced fluorescence showing plasmon-induced ultrafast electronic dynamics in dye molecules

Tamitake Itoh,[1,*] Yuko S. Yamamoto,[1] Hiroharu Tamaru,[2] Vasudevanpillai Biju,[1] Norio Murase,[1] and Yukihiro Ozaki[3]

[1]*Nano-Bioanalysis Research Group, Health Research Institute, National Institute of Advanced Industrial Science and Technology (AIST), Takamatsu, Kagawa 761-0395, Japan*
[2]*Photon Science Center, the University of Tokyo, Tokyo 113-8656, Japan*
[3]*Department of Chemistry, School of Science and Technology, Kwansei Gakuin University, Sanda, Hyogo 669-1337, Japan*

We find unique properties accompanying surface-enhanced fluorescence (SEF) from dye molecules adsorbed on Ag nanoparticle aggregates, which generate surface-enhanced Raman scattering. The properties are observed in excitation laser energy dependence of SEF after excluding plasmonic spectral modulation in SEF. The unique properties are large blue shifts of fluorescence spectra, deviation of ratios between anti-Stokes SEF intensity and Stokes from those of normal fluorescence, super-broadening of Stokes spectra, and returning to original fluorescence by lower energy excitation. We elucidate that these properties are induced by electromagnetic enhancement of radiative decay rates exceeding the vibrational relaxation rates within an electronic excited state, which suggests that molecular electronic dynamics in strong plasmonic fields can be largely deviated from that in free space.

I. INTRODUCTION

Local mode density of electromagnetic (EM) fields near metal nanoparticles (NPs) is enlarged by plasmon resonance, resulting in enhancement or suppression of optical transition rates of molecules close to NP surfaces.[1–10] These phenomena are collectively referred to as EM effects.[11] A broad plasmon resonance line width (∼200 meV) enables EM effects to influence both the excitation and emission transitions of a molecule.[1,3,7,8,10] In the case of a Raman process, this phenomenon is called surface-enhanced Raman scattering (SERS). The SERS cross section of a molecule located inside an NP dimer junction, namely hotspot, exhibits enhancement by a factor of 10^{8-12} (see Refs. [12–16]). The EM effect on SERS has been quantitatively evaluated by investigating the relationship among morphology, plasmon resonance, and SERS using a single Ag NP dimer.[12]

The EM effect also influences fluorescence, namely surface-enhanced fluorescence (SEF) coexisting with SERS. Obtaining a quantitative picture of SEF is more complicated than doing so for SERS, because the decay rate due to energy transfer from excited molecules to metal surfaces is also enhanced by the EM effect.[1–10,17,18] When the enhanced rate of decay of an electronic excited state to the ground state is slower than the vibrational relaxation rate $\sim 10^{12}$ s^{-1}, SEF spectra can be approximately reproduced as fluorescence spectra modulated by radiative plasmon modes, which mean plasmon modes contribute to radiative damping. This type of SEF is called slow dynamic SEF (SDSEF) and has been quantitatively evaluated.[17,18] However, when the enhanced decay rate approaches or exceeds the vibrational relaxation rate, the approximation fails because the SEF from vibrational excited states in an electronic excited state (S_1) cannot be neglected. This type of SEF was called fast dynamic SEF (FD-SEF) and was found as a deviation of luminescence spectra of dye molecules adsorbed on metal surfaces from conventional fluorescence ones.[18,19] In the case of electroluminescence,

FDSEF was investigated as "hot electroluminescence" from a single nanogap between a STM tip and a metal surface.[20] In the case of photoluminescence, FDSEF was preliminary investigated as changes in fluorescence in higher energy spectral regions by Le Ru *et al.*[18] Such investigation of FDSEF is important to clarify the molecular electronic dynamics affected by plasmon resonance on metal surfaces. However, observation of the FDSEF is difficult because SEF spectra are largely modulated by plasmon resonance, which is largely different from hotspot to hotspot.[3,12,17,18] Furthermore, mixing of SDSEF and FDSEF makes the selective observation of FDSEF difficult.

In this paper, we experimentally averaged out the plasmonic modulation in SEF by measurement of large Ag aggregates, which include a large number of hotspots. The spectral properties of SEF were explored. We found excitation laser energy dependence of SEF spectra regarding spectral blue shifts to be ∼400 meV, deviation of ratios between anti-Stokes SEF intensity and Stokes one from those of normal fluorescence, and the super broadening of Stokes regions to be ∼1.0 eV. In the framework of EM effects, the properties are comprehensively explained as direct emission from vibrational excited states in S_1 before the electron relax to the bottom of S_1, that is, FDSEF. These spectral properties are quantitatively reasonable for the systems generating single-molecule SERS, whose EM enhancement is $\sim 10^5$ considering vibrational relaxation rates $\sim 10^{12}$ s^{-1} and electronic relaxation ones $\sim 10^{6-7}$ s^{-1}. Our results show that the widely used description of molecular electronic dynamics is modified in the huge enhanced fields by ultrafast de-excitation due to plasmon resonance.

II. EXPERIMENT

Ag NP colloidal solution was prepared by the reduction of silver nitrate with sodium citrate according to the method reported by Lee and Meisel.[21] The average Ag NP diameter

measured by SEM (JSM-6700F, JEOL) was 40 nm with a small fraction of nonspherical shapes including nanorods. Using an extinction coefficient at the 409 nm plasmon resonance maximum, the colloidal solution had a concentration of 9.6×10^{-11} M. We prepared four kinds of aqueous dye solution, i.e., rhodamine 123 (R123, 1.27×10^{-8} M), rhodamine 6G (R6G, 1.34×10^{-8} M), rhodamine B (RB, 1.30×10^{-8} M), and crystal violet (CV, 1.13×10^{-8} M) solutions containing NaCl (40 mM). We mixed each dye solution with the Ag NP colloidal solution and incubated it for 24 h at room temperature (20 °C). The Ag NPs formed aggregates, and the aggregates grew to have diameters of several hundred micrometers, including dye molecules inside junctions in the NP aggregates. Note that to prepare the Ag NP dimers, we decreased a concentration of NaCl to be ∼10 mM in dye solutions. The surfaces of such Ag NP aggregates were evaluated by scanning electron microscopy (SEM; JSM-6700F, JEOL). The initial dye concentrations are substantially higher than the standard recipe for single-molecule SERS and SEF experiments (∼10^{-10} M).[14,15] However, the effective concentration of dye was extensively reduced by rinsing away most of the dye molecules adsorbed on both Ag aggregates and the glass surfaces using acetone and water; we confirmed that fluorescence signals were never observed from the glass surface. With rinsing, we safely assume that the effective concentrations of the dye in our experiments are equivalent to those for single-molecule SERS and SEF.

The detail of the spectroscopic instrument setup is described elsewhere[22,23] but is briefly described as follows. White light from a 50-W halogen lamp was focused with a dark-field condenser lens to acquire elastic light-scattering spectra from Ag NP aggregates. Elastic light scattering is in principle due to plasmon resonances in the Ag NP aggregates. The spectra due to elastic light scattering are therefore referred to as plasmon resonance spectra hereafter. A cw Ar-ion laser [457.8 nm (2.71 eV), 488 nm (2.54 eV), 514 nm (2.41 eV), 2 W/cm²], a frequency-doubled cw YAG laser [532 nm (2.33 eV), 2 W/cm²], a yellow DPSS cw laser [561 nm (2.21 eV), 2 W/cm²], and a He-Ne laser [633 nm (1.96 eV), 2 W/cm²] were used as the excitation light sources for acquiring the SEF spectra. Both elastic light scattering and SEF spectra were acquired for single Ag NP aggregates dispersed on a glass plate. Note that we confirmed that SEF was exclusively observed from the Ag aggregates, which included dye molecules, and was never observed from Ag aggregates without dye molecules, suggesting that the origin of the observed SEF is exclusively from dye molecules.

III. RESULTS AND DISCUSSION

First, an EM effect on SERS is outlined. The EM effect is composed of both an excitation electric field enhancement $M_{ex}(\omega_{ex})$, $|E_{loc}(\omega_{ex})|/|E_{in}(\omega_{ex})|$ and a Raman emission electric field enhancement $M_{em}(\omega_{em})$, $|E_{loc}(\omega_{em})|/|E_{in}(\omega_{em})|$ by coupling with common radiative plasmon modes, where $|E_{loc}|$ and $|E_{in}|$ are local and incident EM field amplitude, respectively, and ω_{ex} and ω_{em} are excitation and emission angular frequencies, respectively.[1,3,7,8,10,12,16,18] Thus, the orders of both enhancements are similar, and the enhancement factor

of SERS M_{SERS} is

$$|M_{SERS}(\omega_{ex},\omega_{em},d_{av})|^2 = |M_{ex}(\omega_{ex},d_{av})|^2 |M_{em}(\omega_{em},d_{av})|^2,$$
(1)

where d_{av} is the effective distance between a molecule and a metal surface.

Second, an EM effect on SEF is described. The total radiative and nonradiative decay rates of a molecule in a free space are $\Gamma_{r0}(=\int \gamma_{r0}(\omega)d\omega)$ and $\Gamma_{nr0}(=\int \gamma_{nr0}(\omega)d\omega)$, respectively, where $\gamma_{r0}(\omega)d\omega$ and $\gamma_{nr0}(\omega)d\omega$ are the decay rates at ω. The enhancement of a fluorescence excitation rate arises from the coupling of incident EM fields with radiative plasmon modes; thus, the enhancement is common to $|M_{ex}|^2$ in Eq. (1).[3,8,18] However, enhancement of a fluorescence process is not so, because the enhancement of emission arises from the coupling of an excited transition dipole with both radiative and nonradiative plasmon modes.[3,7,8,17,18] The former is the same as $|M_{em}|^2$ in Eq. (1), whereas the latter is not and results in the enhancement of a nonradiative transition rate due to energy transfer from excited transition dipoles to metal surfaces, $|M_{ET}|^2$ (see Refs. 3, 17, and 18). Thus, the spectral density of quantum efficiency of SEF $\eta_{SEF}(\omega_{em})$ is

$$\eta_{SEF}(\omega_{em},d_{av}) = \frac{\gamma_{r0}(\omega_{em})|M_{em}(\omega_{em},d_{av})|^2}{(\Gamma_{Rad} + \Gamma_{ET} + \Gamma_{nr0})},$$
(2)

where Γ_{Rad} is the total enhanced radiative decay rate, given by $\int \gamma_{r0}(\omega)|M_{em}(\omega,d_{av})|^2 d\omega$, and Γ_{ET} is the total enhanced nonradiative decay rate, given by $\int \gamma_{r0}(\omega)|M_{ET}(\omega,d_{av})|^2 d\omega$. Note that plasmons do not affect $\gamma_{nr0}(\omega_{em})$, which is independent of external fields. Thus, the EM enhancement factor of SEF M_{SEF} is

$$|M_{SEF}(\omega_{ex},\omega_{em},d_{av})|^2 = |M_{ex}(\lambda_{ex})|^2 \frac{\eta_{SEF}(\omega_{em},d_{av})}{\eta_0(\omega_{em})}, \quad (3)$$

where $\eta_0(\omega_{em})$ is the spectral density of quantum efficiency of a molecule in a free space and is given by $\gamma_{r0}(\omega_{em})/(\Gamma_{r0} + \Gamma_{nr0})$. In a simple-sphere approximation, dipolar plasmon mode dominates $|M_{em}|^2$; thus, its value varies according to a dipolar field distribution $(1/(1 + d_{av}/R))^6$ (see Refs. 3 and 10), where the NP radius R is much larger than d_{av}. Therefore, $|M_{em}|^2$ is almost constant for small d_{av}. Nonradiative plasmon modes can contribute to M_{ET}; thus, the d_{av} dependence of M_{ET} differs from that of M_{em} in the vicinity of a metal surface. The dependence is predicted as $|M_{ET}|^2 \propto 1/d_{av}^3$ using local EM theory.[3,24] The dependence is typically valid down to $d_{av} \sim 0.5-1$ nm.[3,24] Below the value, a nonlocal theory should be used, one of which predicts the dependence as $1/d_{av}^4$ by assuming a molecule on an infinite flat metal surface.[3,24] Thus, M_{ET} can be much larger than M_{em} for small d_{av}. Indeed, from the ratios of M_{em} to M_{ET}, it is theoretically and experimentally confirmed that $|M_{ET}|^2$ is ∼10^2 times larger than $|M_{em}|^2$ for a molecule showing SM SERS.[3,7,25]

Here, we outline the electronic dynamics in SDSEF and FDSEF. Figure 1(a) shows the potential energy curves of electronic ground and excited states (S_0 and S_1) being separated by ω_0 of a molecule including vibrational states and a corresponding absorption and fluorescence spectrum with vibrational structures. For a molecule, total internal relaxation rate from $S_1(\omega_{ex} - \omega_0)$ to $S_1(0)$ $\Gamma_{int} \sim 10^{12}$ s^{-1} is much faster
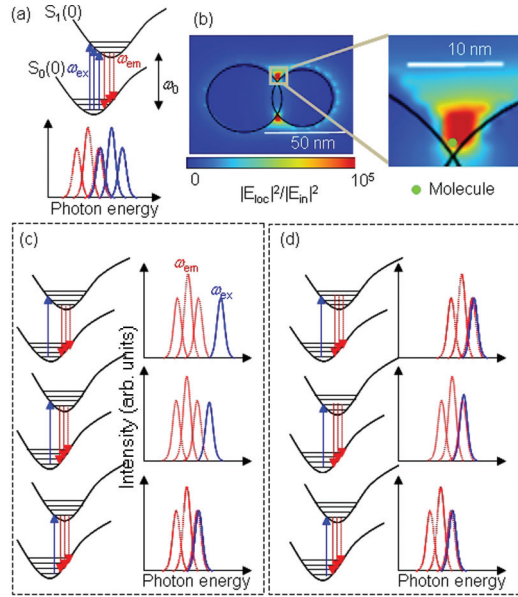
FIG. 1. (Color online) (a) Conventional absorption and fluorescence transition of a molecule in a free space. S_0 and S_1 are electronic ground and excited states with vibrational states, respectively. ω_{ex} and ω_{em} are excitation and emission angular frequencies, respectively. Envelopes of three red bands and three blue bands correspond to fluorescence and absorption spectra, respectively. (b) Distribution of $|E_{loc}|^2/|E_{in}|^2$ around an Ag NP dimer calculated by finite-difference time-domain method and enlarged image of a crevasse of the Ag NP dimer. (c) Excitation laser line (blue lines) dependence of SDSEF transition (red lines). Envelope of three red bands corresponds to SDSEF spectrum (red lines). (d) Excitation laser line (blue lines) dependence of FDSEF transition (red lines). Envelope of three red bands corresponds to FDSEF spectrum (red lines).

than the total decay rate $\Gamma_{r0} + \Gamma_{nr0} \sim 10^{8-9}$ s^{-1}.[3,7,18–20] Thus, the fluorescence spectrum of a molecule in a free space is a radiative transition from $S_1(0)$, which is independent of excitation laser energy. Figure 1(b) shows distribution of $|E_{loc}|^2/|E_{in}|^2$ around an Ag NP dimer. For a molecule located at a position having high local-mode density, such as the dimer junction, Γ_{int} cannot be supposed to be larger than $\Gamma_{Rad} + \Gamma_{ET}$ because $|M_{em}|^2$ reaches 10^5 (see Refs. 3, 7, 8, 12, 14, and 16).

Envelopes of three bands in each left panel in Figs. 1(c) and 1(d) indicate SEF spectra excited with different laser lines. Note that the spectral modulation by radiative plasmon, expressed as $|M_{em}(\omega_{em})|^2$ in Eq. (2), is excluded. Under the condition of SDSEF in Fig. 1(c), namely $\Gamma_{int} \gg \Gamma_{Rad} + \Gamma_{ET} + \Gamma_{nr0}$, excitation and fluorescence transitions are the same as that of a molecule in a free space. Thus, SDSEF spectra can be expressed as a product of $\gamma_{nr0}(\omega_{em})$ and $|M_{em}(\omega_{em}, d_{av})|^2$ (see Refs. 3, 7, 8, and 17). Thus, the spectral density of emission power density of SDSEF $n_{SDSEF}(\omega_{em})$ is

$$n_{SDSEF}(\omega_{em}) = |M_{SEF}(\omega_{ex}, \omega_{em}, d_{av})|^2 \, \sigma_{abs}(\omega_{ex}) \, n_L(\omega_{ex}),$$
(4)

where $n_L(\omega_{ex})$ is the excitation laser power density and $\sigma_{abs}(\omega_{ex})$ is the absorption cross section of a molecule in a free space. Under the condition of FDSEF in Fig. 1(d), namely $\Gamma_{int} < \Gamma_{Rad} + \Gamma_{ET} + \Gamma_{nr0}$, FDSEF cannot be explained in the

same manner as SDSEF, because FDSEF has a component emitting from $S_1(\omega - \omega_0)$, $\omega_0 < \omega < \omega_{ex}$, before relaxing to $S_1(0)$ in Fig. 1. The emission from $S_1(\omega - \omega_0)$ indicates that the highest energy of FDSEF spectra is blue-shifted from fluorescence of a molecule in a free space by $\sim\omega_{ex} - \omega_0$.[18] Thus, $\gamma_{r0}(\omega_{em})$ in Eq. (2) is replaced by $\gamma_{r0}(\omega_{em} - \omega_{ex} + \omega_0)$. In other words, a conventional fluorescence spectrum $\gamma_{r0}(\omega_{em})$ is blue-shifted by $\omega_{ex} - \omega_0$. By taking FDSEF from vibrational excited states $S_1(\omega_{ex} - \omega_0)$ into account, the spectral density of emission power density of FDSEF $n_{FDSEF}(\omega_{em})$ can be approximately expressed as

$$n_{FDSEF}(\omega_{em}) = |M_{ex}(\lambda_{ex})|^2 \, \frac{1}{\eta_0(\omega_{em})}$$
$$\times \frac{\gamma_{r0}(\omega_{em} - \omega_{ex} + \omega_0) \, |M_{em}(\omega_{em}, d_{av})|^2}{(\Gamma_{Rad} + \Gamma_{ET} + \Gamma_{nr0})}$$
$$\times \sigma_{abs}(\omega_{ex}) \, n_L(\omega_{ex}).$$
(5)

Equation (5) and Fig. 1(d) lead us to expect four spectral properties in SEF, shown below, including both SDSEF and FDSEF.

(1) The cutoff energy of FDSEF spectra is ω_{ex} due to emission from $S_1(\omega_{ex} - \omega_0)$, indicating excitation laser energy dependence of cutoff energy.

(2) A rising spectral edge in a higher energy region is similar to that of an absorption spectrum due to emission from $S_1(\omega_{ex} - \omega_0)$; that is, the emission transition shows a trend that is nearly the inverse of that of the absorption transition.

(3) Ratios between anti-Stokes intensity and a Stokes one of FDSEF are determined by a Boltzmann distribution of S_0 because emission transition starts from $S_1(\omega_{ex} - \omega_0)$, indicating the ratios of FDSEF are largely different from those of conventional fluorescence, whose emission transition starts from $S_1(0)$.

(4) FDSEF becomes similar to SDSEF when SEF occurs from $S_1(\omega - \omega_0)$, $\omega_0 \sim \omega$, resulting in spectral super broadening of SEF due to overlapping of FDSEF and SDSEF.

FDSEF is difficult to be explicitly identified because $M_{em}(\omega_{em})$, which differs from NP to NP due to plasmon resonance, largely changes the SEF spectra.[8,17,18] Figures 2(a)– 2(c) shows variations in shapes of Ag NP dimers; plasmon resonance elastic light-scattering spectra, whose shapes are similar to the spectral profiles of radiative plasmon that generates M_{em};[3,18] and SEF spectra of R6G. SEF spectra are largely changed depending on NP dimers and laser energy. The plasmonic modulation prevents us from observing the four properties of FDSEF spectra.

We tried to resolve the plasmonic modulation by the summation of the SEF spectra from a large number of hotspots. Plasmon resonance spectra are largely different from hotspot to hotspot. Thus, the summation makes the spectral shape flat against wavelength and results in averaging out of the plasmonic modulation in the SEF spectra. To carry out the summation, we prepared large Ag NP aggregates containing $\sim 10^{-8}$ M of crystal violet (CV), as shown in Fig. 2(d). The preparation method is described in the experimental section. SEM images show that the NP aggregates contain a large number of junctions that are potential SERS hotspots. The left panels of Fig. 2(e) show SEF images of the aggregate at excitation energies of 2.41 and 2.21 eV. There are many
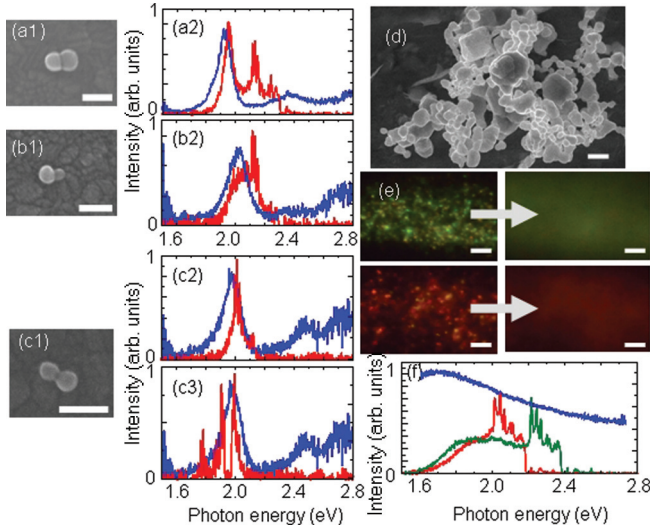
FIG. 2. (Color online) (a1, b1, and c1) SEM images of three Ag dimers showing SERS and SEF activity. (a2 and b2) SEF spectra excited with 2.33 eV (532 nm, red lines) and plasmon resonance spectra (blue lines) from the Ag dimers in (a1 and b1). (c2 and c3) SEF spectra excited with 2.33 eV (532 nm, red lines in c2) and 1.96 eV (633 nm, red lines in c3) and common plasmon resonance spectra (blue lines in c2 and c3) from the Ag dimer in (c1). (d) SEM image of a portion of large Ag NP aggregates. (e) Focused (left panels) and defocused (right panels) SEF images excited with 2.41 eV (514 nm, upper panel) and 2.21 eV (561 nm, lower panel). (f) SEF spectra excited with 2.41 eV (green line) and 2.21 eV (red line), and elastic light-scattering spectra (blue lines) of large Ag NP aggregates. Scale bars are as follows. (a1), (b1), and (c1): 100 nm; (d): 1 μm; and (e): 10 μm.

hotspots with various colors corresponding to spectral maxima of $|M_{em}(\omega_{em})|^2$ s. The large majority of hotspots show intermittent emission, namely blinking, indicating that SEF signals from each hotspot are from single dye molecules. By defocusing the objective lens, the colors are averaged, as shown in the right panels of Fig. 2(e). Figure 2(f) shows averaged SEF spectra from arbitrary points on the aggregates in Fig. 2(e). Due to the averaging, the SEF spectra become quite similar to each other. The similarity indicates that the averaging out of the hotspot-by-hotspot variation in $|M_{em}(\omega_{em})|^2$ was appropriately done.

The averaging out of plasmonic modulation enables us to examine the four properties. Figures 3(a)–3(f) shows SEF spectra of CV excited by five different ω_{ex}s, and Fig. 3(g) shows conventional fluorescence and absorption spectra of molecules in an aqueous solution. Fluorescence of molecules in a free space is independent of ω_{ex} because $\Gamma_{int} \gg \Gamma_{Rad} + \Gamma_{ET} + \Gamma_{nr0}$. However, the measured SEF largely changes spectral shapes depending on ω_{ex}. Each SEF spectrum clearly shows a cutoff energy near ω_{ex}, indicating the first property of FDSEF. This corresponds to blue shifts <400 meV at excitation energy of 2.71 eV. The edge in the higher energy region in Fig. 3(a) is similar to that of an absorption spectrum. The similarity is also noticed in Figs. 3(b)–3(f) around cutoff energy regions by superposing the absorption spectra (black lines) on the SEF spectra, indicating the second property of FDSEF. Ratios between anti-Stokes SEF intensity and Stokes
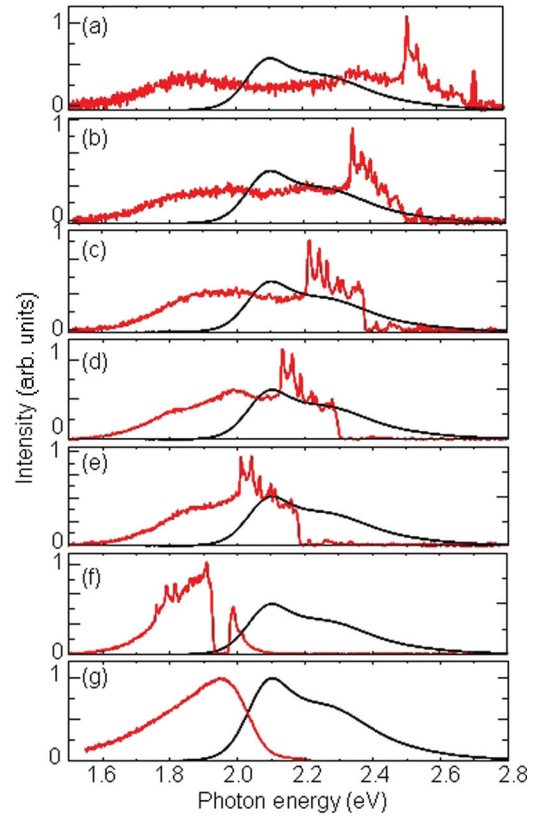

FIG. 3. (Color online) (a–f) Excitation laser energy dependence of SEF spectra of CV from large Ag NP aggregates excited with (a) 2.71, (b) 2.54, (c) 2.41, (d) 2.33, (e) 2.21, and (f) 1.96 eV (red lines) and absorption spectrum of CV molecules in a free space (black lines). Detailed structures around excitation laser lines are SERS bands. (g) Absorption (black line) and fluorescence (red lines) spectrum of CV molecules in aqueous solution ($\sim 10^{-6}$ M).

one are largely deviated from those of normal fluorescence, which is the third property. The SEF spectral tails on the lower energy side are close to the fluorescence spectral tails of molecules in a free space, resulting in super broadening of SEF ~ 1.0 eV, which is the fourth property. This super broadening is evidence of coexistence of FDSEF and SDSEF. It is commonly observed in many reported SERS spectra measured with a broad spectral window.[26] These experimental results are quite consistent with the four predictions, indicating that our evaluation of FDSEF is also valid for the previously studied systems.

To confirm the four spectral properties of FDSEF, we measured SEF of Ag NP aggregates containing three kinds of dye molecules, R123, R6G, and RB, with a concentration of $\sim 10^{-8}$ M. Figure 4(a)–4(c) shows the ω_{ex} dependence of SEF and the fluorescence and absorption spectra of molecules in a free space. The ω_{ex} dependence of cutoff energy and deviation and recovery of anti-Stokes intensity are summarized in Figs. 4(d) and 4(e). Each SEF spectral shape is similar to that of CV and hence clearly exhibits the four properties of FDSEF. These spectral properties indicate the universality of FDSEF as an underlying SERS spectral background. In addition, the recovery of anti-Stokes intensity in Fig. 4(e) due to excitation transition starting from vibrational excited states in S_0 is
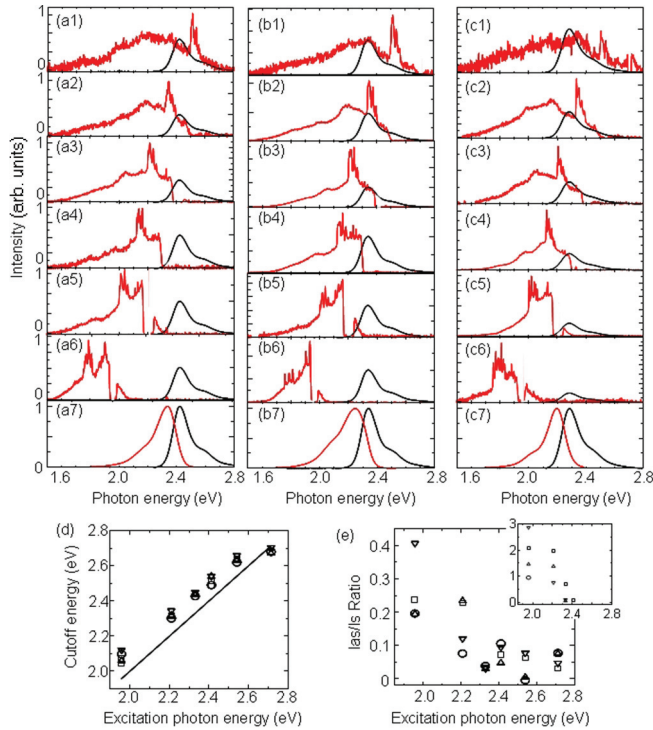
FIG. 4. (Color online) (a–c) Excitation laser energy dependence of SEF spectra of R123 (left panels), R6G (center panels), and Rb (right panels) from large Ag NP aggregates and absorption spectra of each molecule in aqueous solution ($\sim 10^{-6}$ M) (black lines). Detailed structures around excitation laser lines are SERS bands. (d) Excitation photon energy dependence of cutoff energy of SEF spectra for CV ($\circ$), R123 ($\square$), R6G ($\triangle$), and Rb (∇) molecules. (e) Excitation photon energy dependence of ratio of anti-Stokes (with shift from -7.0 to -3.0 meV) to Stokes intensity (with shift from 3.0 to 7.0 meV) of SEF spectra for CV ($\circ$), R123 ($\square$), R6G ($\triangle$), and Rb (∇) molecules. Inset is excitation photon energy dependence of ratio of anti-Stokes to Stokes intensity of fluorescence spectra for CV ($\circ$), R123 ($\square$), R6G ($\triangle$), and Rb (∇) molecules of dye aqueous solution ($\sim 10^{-6}$ M).

commonly observed in lower ω_{ex}. To verify the deviation of ratios between anti-Stokes SEF intensity and Stokes one from those of normal fluorescence, we compared ω_{ex} dependence of ratio of anti-Stokes to Stokes intensity of SEF in Fig. 4(e) with that of conventional fluorescence in the inset of Fig. 4(e). The ratio of SEF is much smaller than that of conventional fluorescence, verifying the drastic deviation. The swelling in SEF spectra around 1.9 eV in Fig. 4(a6)–4(c6) indicates that the distribution of plasmon resonance peaks of $_{hotspot}$s has its maxima at ~ 1.9 eV. Indeed, the plasmon resonance peaks of dimers, which generate the largest EM enhancement, have a maximum around 1.9 eV.[12] Note that to comprehensively examine the universality of the four spectral properties of FDSEF, we need to use dyes emitting fluorescence in the blue and NIR regions.

To examine the mixture of FDSEF and SDSEF, we measured dimer-by-dimer variations in SEF spectra. In SEF measurement of large Ag NP aggregates, both FDSEF and SDSEF signals from dye absorbed on the aggregates are mixed together. In the case of CV with its small quantum yield $\sim 5.2 \times 10^{-5}$ (see Ref. 27), the strong hotspots mainly emit
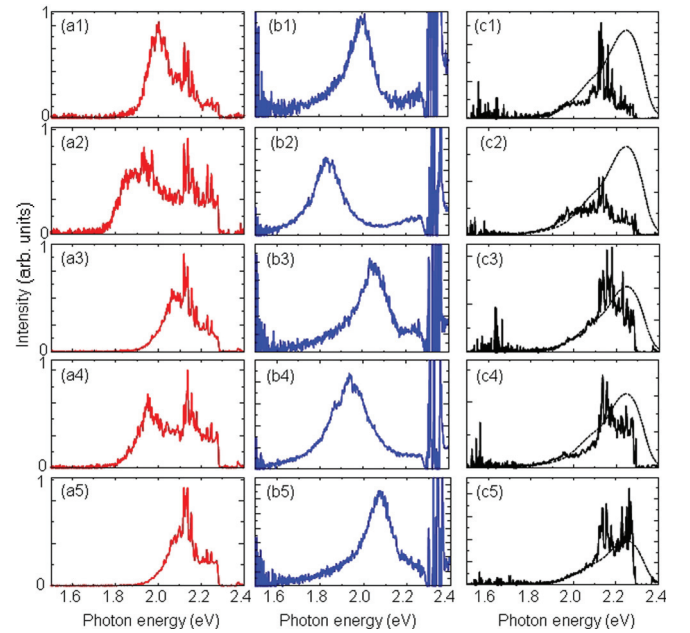

FIG. 5. (Color online) Ag NP dimer-by-dimer variations in (a1–a5) SEF spectra of R6G excited with 2.33 eV, (b1–b5) plasmon resonance spectra. (c1–c5) Ag NP dimer-by-dimer variations in SEF spectra of R6G divided by the plasmon resonance ones. Dotted lines in (c1–c5) are fluorescence spectra of R6G in aqueous solution (10^{-6} M).

FDSEF; however, this is not the case for the rhodamine dyes with high quantum yield ~ 1. In other words, their SEF spectra may largely include SDSEF. To check the expectation, we examined Ag NP dimer-by-dimer variations in SEF spectra of R6G after canceling plasmonic modulation in SEF. Criteria for selection of dimers are described elsewhere.[12] The cancelation was done by dividing a SEF spectrum by plasmon resonance as

$$\sigma_{abs}(\omega_{ex}) \, n_L(\omega_{ex}) = \frac{n_{SDSEF}(\omega_{em})}{|M_{SEF}(\omega_{ex}, \omega_{em}, d_{av})|^2}. \qquad (6)$$

A spectral shape of $|M_{SEF}|^2$ is similar to a plasmon resonance spectrum when a dipolar mode is dominant in $|M_{SEF}|^2$ (see Ref. 8). Thus, we experimentally canceled the plasmonic modulation according to Eq. (6) for many single Ag NP dimers showing dipolar plasmon resonance. Figures 5(a1)– 5(a5), 5(b1)–5(b5), and 5(c1)–5(c5) show typical examples of SEF spectra, plasmon resonance spectra, and SEF spectra divided by the plasmon resonance spectra. SEF spectra in Fig. 5(c1,c2) are largely different from a fluorescence spectrum of dye molecules in solution, indicating that FDSEF contribute mainly to SEF spectra. The SEF spectra in Fig. 5(c5) are similar to the fluorescence spectrum, indicating that SDSEF contribute mainly to the SEF spectra. The SEF spectra in Fig. 5(c3, c4) look intermediate between Fig. 5(c1, c2) and Fig. 5(c5). These results indicate that the SEF spectra of rhodamine dyes from large NP aggregates include both FDSEF and SDSEF.

Here, we discuss the validity of FDSEF regarding the intrinsic limitation of EM enhancement factors. FDSEF requires the value of $>10^4$ for $|M_{em}|^2$ because the molecular decay rates $\sim 10^8$ s^{-1} should be enhanced to exceed the internal relaxation rate $\sim 10^{12}$ s^{-1}. The maximum value of $|M_{em}|^2$ is

generated at a gap between metal NP aggregates and was calculated by Maxwell equations under using nonlocal bulk dielectric functions of metal.[28] The calculated value reaches to $\sim 10^7$, which is high enough to generate FDSEF. However, such values have recently been reconsidered because spilling out of conduction electrons, which loosen the plasmonic field confinement to be $10^{-8}\lambda^3$, where λ is a wavelength on the metal surfaces, makes the maximum value of $|M_{em}|^2$ lower than the calculated value by a factor of 10^2 (see Refs. [29] and [30]). Indeed, experimental evaluations demonstrated that $|M_{em}|^2$ does not exceed $\sim 10^5$ using many Ag NP dimers and nanorods.[8,12,31,32] This fact indicates that FDSEF is realistic for NP aggregates showing the strongest SERS activity but not so for the other systems, for example, isolated NPs and flat metal surfaces.

In conclusion, we have demonstrated the experimental evidence for fast dynamics in the SEF, which is commonly observed as broad background emission of SERS, of dye molecules adsorbed on Ag NP aggregates by comparing conventional fluorescence spectra with SEF spectra from which plasmonic-spectral modulation was excluded. We have found that SEF exhibits cutoff energy, drastic changes of anti-Stokes to Stokes intensity ratios, and super broadening of Stokes spectra. The excitation energy dependence of SEF demonstrates that both suppression and broadening are induced by the enhancement of radiative decay rates such that they become greater than the vibrational relaxation rates, resulting in emission from vibrational excited states. Our results are important for not only the understanding, prediction, and control of molecular electronic dynamics near metal nanostructures but also the development of EM strong coupling systems composed of molecules using quantum electrodynamics. Such systems may provide new insights into the coupling among electrons, excitons, plasmons, and photons.

*Corresponding author: tamitake-itou@aist.go.jp

[1] B. Pettinger, J. Chem. Phys. **85**, 7442 (1986).

[2] E. Dulkeith, A. C. Morteani, T. Niedereichholz, T. A. Klar, J. Feldmann, S. A. Levi, F. C. J. M. van Veggel, D. N. Reinhoudt, M. Möller, and D. I. Gittins, Phys. Rev. Lett. **89**, 203002 (2002).

[3] P. Johansson, H. Xu, and M. Käll, Phys. Rev. B **72**, 035427 (2005).

[4] P. Anger, P. Bharadwaj, and L. Novotny, Phys. Rev. Lett. **96**, 113002 (2006).

[5] F. Tam, G. P. Goodrich, B. R. Johnson, and N. J. Halas, Nano Lett. **7**, 496 (2006).

[6] V. Yannopapas, E. Paspalakis, and N. V. Vitanov, Phys. Rev. Lett. **103**, 063602 (2009).

[7] C. M. Galloway, P. G. Etchegoin, and E. C. Le Ru, Phys. Rev. Lett. **103**, 063003 (2009).

[8] K. Yoshida, T. Itoh, V. Biju, M. Ishikawa, and Y. Ozaki, Phys. Rev. B **79**, 085419 (2009).

[9] C. Vandenbem, D. Brayer, L. S. Froufe-Pérez, and R. Carminati, Phys. Rev. B **81**, 085444 (2010).

[10] G. Sun and J. B. Khurgin, Phys. Rev. A **85**, 063410 (2012).

[11] E. M. Purcell, Phys. Rev. **69**, 681 (1946).

[12] K. Yoshida, T. Itoh, H. Tamaru, V. Biju, M. Ishikawa, and Y. Ozaki, Phys. Rev. B **81**, 115406 (2010).

[13] K. Imura, H. Okamoto, M. Hossain, and M. Kitajima, Nano Lett. **6**, 2173 (2006).

[14] K. Kneipp, Y. Wang, H. Kneipp, L. Perelman, I. Itzkan, R. R. Dasari, and M. Feld, Phys. Rev. Lett. **78**, 1667 (1997).

[15] S. M. Nie and S. Emory, Science **275**, 1102 (1997).

[16] H. Xu, E. Bjerneld, M. Käll, and L. Borjesson, Phys. Rev. Lett. **83**, 4357 (1999).

[17] M. Ringler, A. Schwemer, M. Wunderlich, A. Nichtl, K. Kürzinger, T. A. Klar, and J. Feldmann, Phys. Rev. Lett. **100**, 203002 (2008).

[18] E. C. Le Ru, P. G. Etchegoin, J. Grand, N. Félidj, J. Aubard, and G. Lévi, J. Phys. Chem. C **111**, 16076 (2007).

[19] G. Ritchie and E. Burstein, Phys. Rev. B **24**, 4843 (1981).

[20] Z. C. Dong, X. L. Zhang, H. Y. Gao, Y. Luo, C. Zhang, L. G. Chen, R. Zhang, X. Tao, Y. Zhang, J. L. Yang, and J. G. Hou, Nat. Photonics **4**, 50 (2010).

[21] P. Lee and D. Misel, J. Phys. Chem. **86**, 3391 (1982).

[22] T. Itoh, K. Hashimoto, and Y. Ozaki, Appl. Phys. Lett. **83**, 2274 (2003).

[23] T. Itoh, Y. Kikkawa, K. Yoshida, K. Hashimoto, V. Biju, M. Ishikawa, and Y. Ozaki, J. Photochem. Photobio. A **183**, 322 (2006).

[24] I. A. Larkin, M. I. Stockman, M. Achermann, and V. I. Klimov, Phys. Rev. B **69**, 121403 (2004).

[25] T. Itoh, M. Iga, H. Tamaru, K. Yoshida, V. Biju, and M. Ishikawa, J. Chem. Phys. **136**, 024703 (2012).

[26] For example, T. Itoh, K. Hashimoto, V. Biju, M. Ishikawa, and Y. Ozaki, J. Phys. Chem. B **110**, 9579 (2006).

[27] M. S. Baptista and G. L. Indig, J. Phys. Chem. B **102**, 4678 (1998).

[28] H. Xu, J. Aizpurua, M. Käll, and P. Apell, Phys. Rev. E **62**, 4318 (2000).

[29] R. Esteban, A. G. Borisov, P. Nordlander, and J. Aizpurua, Nat. Commun. **3**, 825 (2012).

[30] K. J. Savage, M. M. Hawkeye, R. Esteban, A. G. Borisov, J. Aizpurua, and J. J. Baumberg, Nature **491**, 574 (2012).

[31] K. J. Russell, T. L. Liu, S. Cui, and E. L. Hu, Nat. Photonics **6**, 459 (2012).

[32] T. Itoh, H. Yoshikawa, K. Yoshida, V. Biju, and M. Ishikawa, J. Chem. Phys. **130**, 214706 (2009).